Journal of Hydrology 557 (2018) 448–459

Contents lists available at ScienceDirect

Journal of Hydrology

journal homepage: www.elsevier.com/locate/jhydrol

Research papers

The cumulative effects of forest disturbance and climate variability on streamflow components in a large forest-dominated watershed

Qiang Li [a], Xiaohua Wei [a,*], Mingfang Zhang [b], Wenfei Liu [c], Krysta Giles-Hansen [a], Yi Wang [a]

[a] Department of Earth, Environmental and Geographic Sciences, University of British Columbia Okanagan, 1177 Research Road, Kelowna, British Columbia V1V 1V7, Canada
[b] School of Resources and Environment, University of Electronic Science and Technology of China, 2006 Xiyuan Ave., Chengdu 611731, China
[c] Institute of Ecology and Environmental Science, Nanchang Institute of Technology, Nanchang, China

ARTICLE INFO

Article history:
Received 8 February 2017
Received in revised form 18 December 2017
Accepted 21 December 2017
Available online 21 December 2017
This manuscript was handled by T. McVicar, Editor-in-Chief, with the assistance of Shengping Wang, Associate Editor

Keywords:
Forest disturbance
Climate variability
Baseflow separation
Relative contributions
Streamflow components
Cumulative effects

ABSTRACT

Assessing how forest disturbance and climate variability affect streamflow components is critical for watershed management, ecosystem protection, and engineering design. Previous studies have mainly evaluated the effects of forest disturbance on total streamflow, rarely with attention given to its components (e.g., base flow and surface runoff), particularly in large watersheds (>1000 km^2). In this study, the Upper Similkameen River watershed (1810 km^2), an international watershed situated between Canada and the USA, was selected to examine how forest disturbance and climate variability interactively affect total streamflow, baseflow, and surface runoff. Baseflow was separated using a combination of the recursive digital filter method and conductivity mass balance method. Time series analysis and modified double mass curves were then employed to quantitatively separate the relative contributions of forest disturbance and climate variability to each streamflow component. Our results showed that average annual baseflow and baseflow index (baseflow/streamflow) were 113.3 ± 35.6 mm year^{-1} and 0.27 for 1954–2013, respectively. Forest disturbance increased annual streamflow, baseflow, and surface runoff of 27.7 ± 13.7 mm, 7.4 ± 3.6 mm, and 18.4 ± 12.9 mm, respectively, with its relative contributions to the changes in respective streamflow components being 27.0 ± 23.0%, 29.2 ± 23.1%, and 25.7 ± 23.4%, respectively. In contrast, climate variability decreased them by 74.9 ± 13.7 mm, 17.9 ± 3.6 mm, and 53.3 ± 12.9 mm, respectively, with its relative contributions to the changes in respective streamflow components being 73.0 ± 23.0%, 70.8 ± 23.1% and 73.1 ± 23.4%, respectively. Despite working in opposite ways, the impacts of climate variability on annual streamflow, baseflow, and surface runoff were of a much greater magnitude than forest disturbance impacts. This study has important implications for the protection of aquatic habitat, engineering design, and watershed planning in the context of future forest disturbance and climate change.

© 2017 Elsevier B.V. All rights reserved.

1. Introduction

The impacts of changes in forest cover on water yield have long been investigated across the globe (Andréassian, 2004; Brown et al., 2005; Farley et al., 2005; Stednick, 1996; Wei et al., 2013; Wei et al., 2017). Recent reviews on the relationship between forest change and water yield across multiple spatial scales have concluded that deforestation increases water yield, while reforestation decreases it (Li et al., 2017; Zhang et al., 2017a). The implications of these reviews are pivotal for water supply, ecosystem protection, and engineering design. However, previous studies have mainly focused on how forest change affects total streamflow with limited attention given to major streamflow components (i.e., baseflow and surface runoff). Considering all streamflow components can lead to a more complete understanding of hydrological responses to forest change in a watershed.

Limited studies have examined the impacts of change in forest cover or land use on baseflow and surface runoff. A global summary on this subject with watershed sizes ranging from plot level (≪1 ha) to large watershed scale (>1000 km^2) is provided in Table 1. In small watersheds (<100 km^2), the impacts of change in forest cover on baseflow or groundwater recharge are mainly inferred from the change in groundwater table with relatively consistent conclusions. For example, a rising of the groundwater table was observed after forest logging, indicating forest disturbance increased groundwater recharge or baseflow (Table 1; Smerdon et al., 2009), while streamflow dried up completely in the ninth

* Corresponding author.
E-mail address: adam.wei@ubc.ca (X. Wei).

https://doi.org/10.1016/j.jhydrol.2017.12.056
0022-1694/© 2017 Elsevier B.V. All rights reserved.

Table 1
A global summary of the effects of change in land cover on all streamflow components including total streamflow, baseflow, and surface runoff with a focus on baseflow or groundwater (MAP: mean annual precipitation).

No.	Source	Study site	Country	MAP (mm)	Area (ha)	Land cover change type	Changes in groundwater table, recharge, or baseflow
1	Ahiablame et al. (2017)	Missouri River (99 stations)	USA	255–1140	135,000,000	Agriculture land expansion	Every 1% of the agriculture land expansion led to 0.2% decrease in baseflow
2	Barnett (1990)	Murray River Basin	South Australia	300	–	Land conversion from native mallee to crop	Groundwater recharge increased from <0.1-0.2 mm/year to 3–30 mm/year as a result of land conversion
3	Bent (2001)	Cadwell Creek	Massachusetts, USA	1174	–	34% of partial clearcut	Groundwater recharge increased by 68 mm/year for six seasons following harvest
4	Bliss and Comerford (2002)	Gainesville	Florida, USA	1150	42	Clear-cut	A 21–49 cm rise in groundwater table was detected after 900 days of treatment
5	Calder et al. (1992)	Karnataka	Southern India	800	–	Reforestation	Groundwater recharge reduced by eucalyptus plantations
6	Cao et al. (2009)	Motueka River Catchment	New Zealand	–	218,000	Pine planation	Pine planation reduced total streamflow (4.5%), baseflow (4.5%), and surface runoff (3.4%)
7	Cook et al. (1989)	Western Murray Basin	South Australia	340	14	Clear-cut	Groundwater recharge increased by 20 mm/year
8	Dubé et al. (1995)	St. Lawrence Low lands	Quebec, Canada	957	Forest stands (<1 ha)	Clear-cut	A 7–52 cm rise in groundwater table was found
9	Evans et al. (2000)	Moose Lake	Alberta, Canada	468	2.7	Clear-cut	Groundwater table was 26 cm higher in cut area compared to uncut area
10	Fannin et al. (2000)	Carnation Creek	British Columbia, Canada	2100–4800	12	90% of clear-cut	A 50–150 cm rise in groundwater table was found in cut area
11	Hetherington (1998)	Carnation Creek	British Columbia, Canada	2100–4801	1000	41% of clear-cut	A 30–50 cm rise in groundwater table was detected after 10 years following harvest
12	Huang et al. (2016)	Upper Du watershed	China	728–1480	896,100	Conversion of 5.3% farmland to forest	Reforestation is a major factor with the negative impacts on baseflow
13	Khoi and Suetsugi (2014)	Be River watershed	Vietnam	2400	750,000	16.3% of deforestation	An increase in streamflow (0.2 to 0.4%) and surface runoff (4.8 to 10.7%), meanwhile, a decrease in baseflow (3.5 to 7.9%) were found
14	Leduc et al. (2001)	Niamey	Southwestern Niger	565	–	Land conversion of native savannah to millet field	Groundwater table was risen 0.01–0.45 m/year by land conversion of native savannah to millet field
15	Ma et al. (2009)	Kejie watershed	Southwestern China	967	175,500	Reforestation	An increase in baseflow and a decrease in surface runoff and streamflow were detected
16	Marcotte et al. (2008)	St. Lawrence Low lands	Quebec, Canada	1126	Forest stands (<1 ha)	Clear-cut	An increase in groundwater table of 50–70 mm higher than pre-disturbance level after 10 years of clearcut, but had reached nearly 50% of pre-cut level
17	Megahan and Clayton (1983)	Pine Creek	Idaho, USA	890	0.97	63% clear-cut and burned	A 90 cm rise in the groundwater table, and decreasing to 40 cm after 2 years were detected
18	Mishra et al. (2010)	Wisconsin	USA	710–866	16,964,000	30% of deciduous forest convert to agricultural land	Annual surface runoff and baseflow increased of 40.4 mm and 469.1 mm, respectively
19	Nepstad et al. (1994)	Amazon River Basin	Pará, Brazil	1750	–	Land conversion of evergreen tropical forest to pasture	An increment of 370 mm was found in plant available soil water
20	Peck and Williamson (1987)	Collie River Basin (5 watersheds)	Western Australia	820–1120	80–350	Clear-cut and partially cut	Water table increased by 260 cm/year in clear-cut area and 90 cm/year in partial clear-cut area
21	Pothier et al. (2003)	St. Lawrence Low lands	Quebec, Canada	510	Forest stands (<1 ha)	Clear-cut and partially cut	Up to 22 cm rise in groundwater table was found
22	Salama et al. (1993)	Cuballing Catchments	Southwestern Australia	462	175	70% of land conversion of native eucalypt forest by grass land	Groundwater recharge increased from 0.4 -1.0 mm to 10–25 mm
23	Schofield and Bari (1991)	Collie River Basin	Western Australia	713	127	35% of reforestation	Groundwater level declined an average 1.47 m after a 10 year period of reforestation
24	Scott and Lesch (1997)	Mokobulaan experimental catchments	South Africa	1135	26.2	100% of reforestation	Streamflow dried up completely in the ninth year after *Eucalyptus grandis* plantation
25	Scott and Lesch (1997)	Mokobulaan experimental catchments	South Africa	1135	34.6	100% of reforestation	Streamflow dried up completely in the twelfth year after *Pinus patula* plantation
26	Shi et al. (2013)	Xixian Basin	China	1145	1,019,100	2.38% and 10.33% expand in forest and paddy area	Land cover change decreased surface runoff (1.6%), baseflow (2.8%), and streamflow (2.1%)
27	Urie (1971)	–	Michigan, USA	790	16.2	50% of partially cut	A 100 cm rise as a result of higher snowpack
28	Xu et al. (2013)	Iowa, Illinois, Indiana, and Ohio (55 stations)	Midwest USA	966	5700–102,600	Agriculture land expansion	Land surface change contributed more to baseflow (74%) than climatic variability (27%) in 20/55 watersheds

(*continued on next page*)

Table 1 (*continued*)

No.	Source	Study site	Country	MAP (mm)	Area (ha)	Land cover change type	Changes in groundwater table, recharge, or baseflow
29	Zhang and Schilling (2006)	Mississippi River Basin (16 watersheds)	USA	724–907	136,200–4,366,980	Conversion of perennial vegetation to seasonal row crops	Baseflow and streamflow were increased
30	Zhang et al. (2016)	Heihe River Basin	China	450	12,800,000	Conversion of 17.1% and 0.5% deduction in farmland and forest to Urbanization	Reductions in surface runoff (−0.89%), baseflow (−0.54%), and streamflow (−0.31%) were detected
31	Zhou et al. (2013)	Xitiaoxi Basin	China	1466	137,100	5.9% of decrease in forest and 178% of increase in urban area	Surface runoff was increased 11.3%, and baseflow decreased by 11.2%
32	This study	Upper Similkameen River watershed	British Columbia, Canada	889	181,000	37% of forest disturbance	Forest disturbance increased streamflow (27.7 mm), baseflow (7.4 mm), and surface runoff (18.4 mm)

year after Eucalyptus plantation in South Africa (Scott and Lesch, 1997), demonstrating that an increase in forest cover decreased baseflow. For large watersheds (>1000 km^2), hydrological models were often adopted to study the effects of forest change on streamflow components, and the conclusions from those model-based studies were inconsistent (Khoi and Suetsugi, 2014; Ma et al., 2009; Zhang et al., 2016; Zhou et al., 2013). For instance, vegetation expansion has dramatically reduced total streamflow and surface runoff, but baseflow was increased using the Soil and Water Assessment Tool (SWAT) in the Kejie watershed (1755 km^2), Southwestern China (Ma et al., 2009). Conversely, Khoi and Suetsugi (2014) concluded that a reduction in forest cover augmented total streamflow and surface runoff, while decreased baseflow in the Be River catchment (7500 km^2), Vietnam. These contrasting results highlight large variations in hydrological responses of streamflow components, especially baseflow alteration due to forest or land cover change. The limited studies, along with inconsistent results in large watersheds, demonstrate that more case studies are needed.

In large forested watersheds, forest change and climate variability are two major drivers influencing hydrological variation. To investigate the impacts of forest change on hydrology, the effects of climate variability on flow must be either removed or taken into consideration. The interest in considering both drivers and their relative contributions to streamflow has been growing significantly (e.g., Li et al., 2017; Wei et al., 2013; Zhang et al., 2008; Wei et al., 2017). However, a direct and quantitative assessment of how annual streamflow responds to both forest change and climate variability is challenging, particularly in large watersheds as it requires explicit consideration of climate variability when assessing the hydrological effects of forest change (Wei and Zhang, 2010; Zhang et al., 2012). It is even more challenging to study the relative contributions of climate variability and forest change to all streamflow components.

Advanced statistical analyses have been used to explore the effects of land cover or forest change on total streamflow. For example, statistical techniques such as the sensitivity-based method, double mass curves, simple water balance, and the time trend method have been developed and widely used (Wei et al., 2013). Among them, Wei and Zhang (2010) devised modified double mass curves (MDMC) and time series analysis to separate the relative contributions of forest change and climate variability to annual streamflow. As the MDMC method is based on water balance, it has the potential to separate the relative effects of forest change and climate variability on baseflow and surface runoff.

Another challenge in this research subject is the accurate separation of baseflow from total streamflow. Numerous methods have been developed to separate total streamflow into baseflow and surface runoff (Zhang et al., 2013). Among them, the conductivity mass balance (CMB) method has received growing attention because: 1) it is developed based on the close correlation between discharge and water specific conductance (referred to as conductivity hereafter). In theory, baseflow percolates through soil and rock and therefore picks up more ions on its route than surface runoff, which leads to higher ion concentrations than surface runoff (Matsubayashi et al., 1993; Stewart et al., 2007); and 2) conductivity data are easy to obtain with moderate cost. However, CMB applications are often constrained by long-term daily conductivity data. To address this shortcoming, Zhang et al. (2013) developed a combined baseflow separation method, which used the CMB method to calibrate the recursive digital filter method. In this way, long-term baseflow can be accurately separated. In this combined method, Li et al. (2014) found that a minimum of 6-months continuous conductivity data in low flow seasons (e.g., summer) should be collected to assure its reliability.

Based on our literature review, the hypothesis of this study was that for a large forested watershed located in a snow-dominated hydrological regime, forest disturbance has significant effects on streamflow and its components. Our specific key objectives of this study were: 1) to explore the effects of forest disturbance on total streamflow, baseflow, and surface runoff in the Upper Similkameen River watershed; 2) to quantify the relative contributions of forest disturbance and climate variability to total streamflow, baseflow, and surface runoff; and 3) to discuss possible implications of our results for management of water resource and protection of aquatic functions.

2. Study site and data

2.1. Study site

The Upper Similkameen River (USR) watershed has a drainage area of 1810 km^2, of which 540 km^2 is located in Washington, USA. The headwaters of the watershed are on the USA side of the border draining north into Canada (Fig. 1). Elevation ranges from 635 to 2546 m above sea level. In 1954–2013, the average annual precipitation was 1000 mm. The highest and lowest monthly mean temperatures were 19.6 °C in July and −9.7 °C in January. The watershed covers several biogeoclimatic zones including the Interior Douglas Fir zone on the valley floors and the Montane Spruce and the Engelmann Spruce-Subalpine Fir at higher elevations (Pojar et al., 1987).

2.2. Watershed data

2.2.1. Climate data

Monthly mean (T_{mean}), maximum (T_{max}), and minimum (T_{min}) temperatures, and precipitation of the study watershed were generated from the Climate West North American (WNA) dataset for

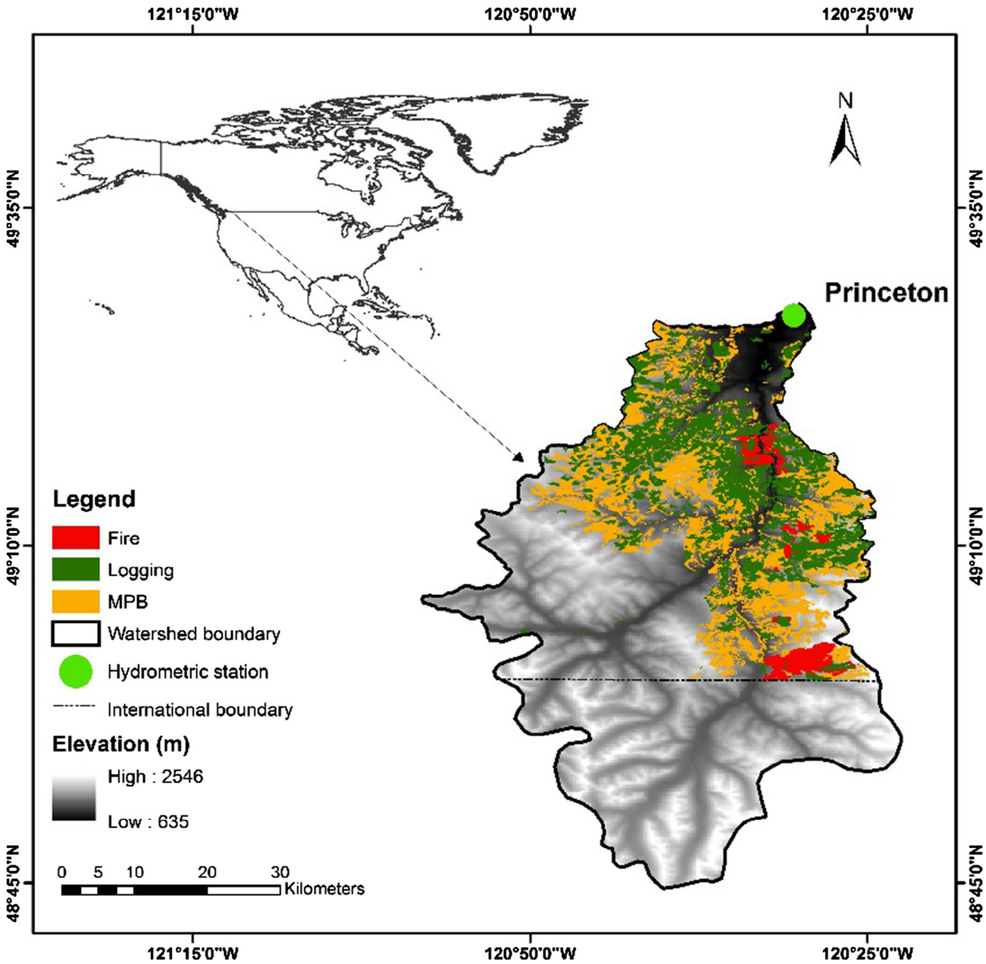

Fig. 1. Locations, elevations, and spatial distributions of forest disturbance (fire, logging, and mountain pine beetle (MPB) infestation) in the Upper Similkameen River watershed with a total area of 1810 km^2, of which 530 km^2 is in Washington State, USA. (*Note*: The upper reaches of the watershed are mainly located in the conservation parks where logging is prohibited).

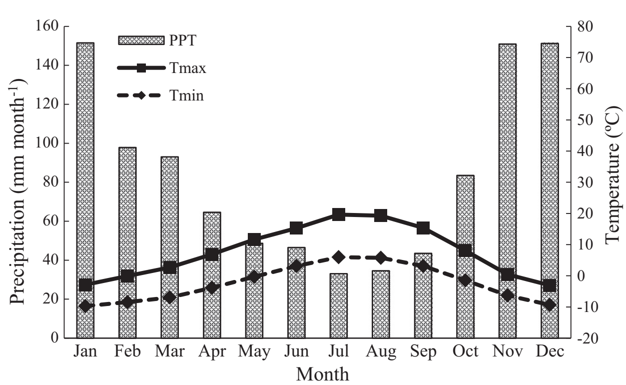

Fig. 2. Long-term (1954–2013) mean monthly precipitation, monthly maximum (T_{max}) and minimum (T_{min}) temperatures in the Upper Similkameen River watershed.

1954–2013 (Wang et al., 2016). ClimateWNA is a standalone program that extracts and downscales historical climate data from Climate Research Unit at the University of East Anglia (Mitchell and Jones, 2005) from 1901 to 2014 (Wang et al., 2016). It calculates monthly and annual climate variables for any given location based on latitude, longitude, and elevation. Given the large spatial variations in climate across the watershed, monthly climate data were generated at a resolution of 500 × 500 m across the study watershed (Fig. 2).

2.2.2. Forest disturbance data

Two provincial-level databases were obtained from the British Columbia Ministry of Forests, Lands and Natural Resources Operations: the Cutblocks 2010 and the Vegetation Resources Inventory (VRI) 2010. The Cutblocks database is a spatial record of forest harvest size, location, and timing. The VRI database provides detailed tree characteristics and additional non-logging disturbance type (i.e. fire and insect infestation). Therefore, these two databases are complementary, and were both used to quantify the forest disturbance history in the study watershed. It should be noted that forest disturbance data are not available in the part of the watershed located in the USA. The quantification of forest disturbance was only made in the Canadian portion of the watershed.

2.2.3. Hydrology and conductivity data

Daily stream discharge data were collected from the hydrometric station (Station ID: 08NL007, Similkameen River at Princeton) that is operated and maintained by Environment Canada. The annual average discharge was 423 mm in 1954–2013. Agricultural irrigation was the largest water consumer in the watershed, and accounted for less than 2% of the annual mean flow (Summit, 2011). The highest discharge occurred in the snow-melting season (March to May), accounting for 68% of the annual discharge. The in-situ conductivity probe (CTD-Diver, DI 271, Schlumberger Water Service, Canada) was installed near the hydrometric station to measure continuous conductivity at a frequency of 30 min from

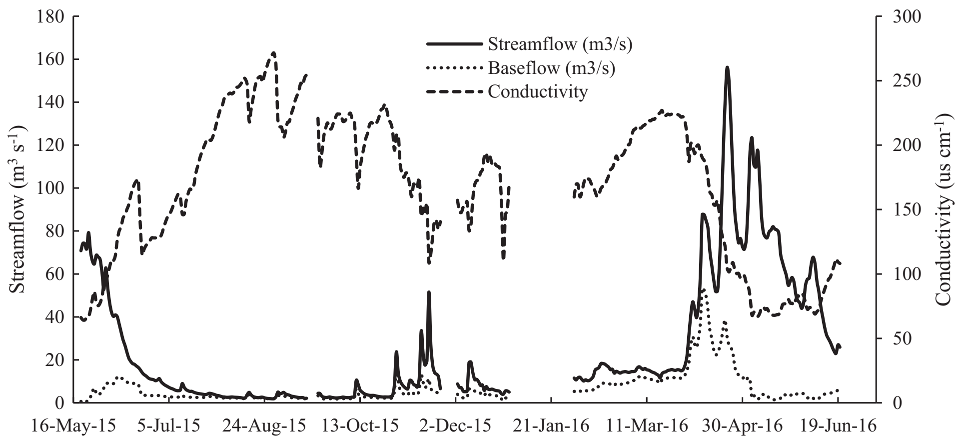

Fig. 3. Measured conductivity and streamflow, and separated baseflow using conductivity mass balance method from May 19, 2015 to June 21, 2016 in the Upper Similkameen River watershed.

May 19, 2015, to June 21, 2016. The conductivity measurements for each day were averaged to derive daily conductivity (Fig. 3).

3. Methods

3.1. Quantification of forest disturbance levels

Logging, mountain pine beetle (MPB) infestation, and wildfire are the three major forest disturbance types in the study watershed (Fig. 4). According to the VRI database, a forest stand in the study watershed was either disturbed by only one type (e.g., logging or wildfire or MPB), or two types of disturbances where a forest stand that was first disturbed by one type and was followed by another (e.g., a forest stand that is disturbed by wildfire first and then by salvage logging).

Different kinds of forest disturbance cumulate over space and time in any forested watersheds. Equivalent clear-cut area (ECA) is used to quantify forest disturbance levels and is defined as the area that has been clear-cut, fire-killed, or infested by MPB, with a reduction factor (ECA coefficient) to account for hydrological recovery due to forest regeneration. An ECA coefficient of 100% means that there is no hydrological recovery in a disturbed area, while an ECA coefficient of zero indicates a full hydrological recovery. The cumulative equivalent clear-cut area (CECA) is the sum of annual ECA values in the watershed. The hydrological recovery of a forest stand is related to its growth rate over time and is therefore determined by many factors including disturbance type, climate, and tree species. A detailed description of the ECA estimation procedure can be found in Wei and Zhang (2010).

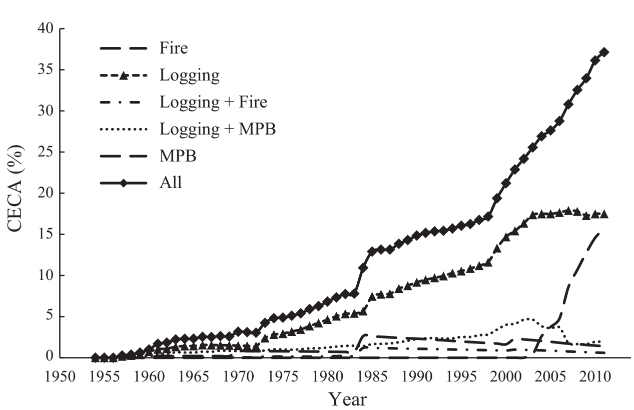

Fig. 4. Cumulative equivalent clear-cut areas (CECA) (%) of the Upper Similkameen River from 1954 to 2011.

Logging or post-disturbance salvage logging was the dominant disturbance type in the USR watershed over the study period. The upper reaches of the watershed are in the E.C. Manning Provincial Park, Canada where logging is prohibited (Fig. 1). The average annual area logged was 0.38% of the watershed area. The CECA from logging was 17.5% of the watershed area in 1954–2011. Forest fire occasionally occurred with the largest forest fire occurring in 1984. On average, 1% of the watershed area was burnt annually. MPB was not a significant disturbance type until 2003. About 1.4% and 2.3% of the watershed area were affected by MPB in 2004 and 2007, respectively. In 2011, the CECA from MPB reached 15.7% of the watershed area. In summary, the total CECA from all disturbance types was 37.1% of the total watershed area in 2011 (Fig. 4).

3.2. Baseflow separation methods

3.2.1. Conductivity mass balance (CMB) method

The conductivity mass balance (CMB) method (Stewart et al., 2007) is expressed as:

$$BF = Q\frac{C_q - C_{ro}}{C_{bf} - C_{ro}} \tag{1}$$

where, BF is baseflow (m^3 s^{-1}), Q is daily streamflow discharge (m^3 s^{-1}), C_q is the conductivity of streamflow (μS cm^{-1}), C_{bf} is the conductivity of baseflow (μS cm^{-1}), and C_{ro} is the conductivity of surface runoff (μS cm^{-1}). C_{ro} is assumed to correspond to the highest daily streamflow, while C_{bf} corresponds to the lowest daily streamflow. Assumptions of applying the CMB method are: 1) contributions from other streamflow components are negligible; 2) C_{bf} and C_{ro} are constant over the specific period; and 3) C_{bf} and C_{ro} values are different from each other as baseflow percolates through soil and rocks, and carries more ions on its route, and thus has higher conductivity than surface runoff (Li et al., 2014; Miller et al., 2014; Stewart et al., 2007).

3.2.2. Recursive digital filter (RDF) method

The recursive digital filter (RDF) method (Eq. (2)) proposed by Eckhardt (2005) was used for the long-term baseflow separation in this study.

$$BF_t = \frac{(1 - BFI_{\max})\alpha BF_{t-1} + (1 - \alpha)BFI_{\max}Q_t}{1 - \alpha BFI_{\max}} \tag{2}$$

Subject to $BF_t < Q_t$, where, BF is baseflow ($m^3 s^{-1}$); Q is daily streamflow discharge ($m^3 s^{-1}$); α is recession constant (dimensionless) and BFI_{max} is the maximum value of the baseflow index (the ratio of baseflow to total streamflow). In the RDF method, α can be determined from the hydrograph. However, BFI_{max} cannot be directly measured (Li et al., 2014). The accuracy of the baseflow results from the RDF method is more sensitive to the BFI_{max} than to the recession constant. The BFI_{max} should normally be estimated from a tracer method (Zhang et al., 2013; Zhang et al., 2017a). In this study, the BFI calculated from the CMB method was used as the initial value of BFI_{max} in the RDF method. Then, the recession constant α and BFI_{max} were adjusted to minimize the residuals of total baseflow between the RDF and CMB. The baseflow separated by paired α and BFI_{max} with minimum residuals compared to that by the CMB method were determined as the final parameters for the RDF method (Li et al., 2014; Zhang et al., 2013). The calibrated RDF method was finally employed to separate the long-term baseflow (1954–2013) for the study watershed.

3.3. Cross-correlations analysis

Cross-correlation analysis is an effective method to test whether there are significant relationships among time series variables. Its advantage is that it can remove autocorrelations existing in data series and identify lagged causality between two data series (Zhang and Wei, 2014). In this study, cross-correlation was used to detect the relationships and lagged effects between CECA and annual streamflow, baseflow, and surface runoff. All of the tested hydrological variables and CECA data were pre-whitened to remove autocorrelation by fitting ARIMA (Autoregressive Integrated Moving Average) models. Model residuals from the ARIMA model with the best performance, achievement of model stationary, and coefficient of determination were selected for cross-correlation analysis (Liu et al., 2015a).

3.4. Quantification of the relative contributions of forest disturbance and climate variability to streamflow components

Forest disturbance and climate variability are commonly considered two major drivers for hydrological variations in large forested watersheds. Modified double mass curves (MDMC) have been used to quantify the relative contributions of forest disturbance and climate variability to annual streamflow (Liu et al., 2015a; Yao et al., 2012; Zhang et al., 2012). To quantify the relative contributions of forest disturbance and climate variability to annual total streamflow, baseflow, and surface runoff, respectively, we applied the same approach as for annual streamflow.

The basic assumption of MDMC is that a linear relationship is assumed between cumulative effective annual precipitation (P_{ae}) and cumulative annual total streamflow (Q_a), baseflow (BF_a), and surface runoff (SR_a) (Liu et al., 2015a; Wei and Zhang, 2010; Zhang et al., 2012, 2017c; Zheng et al., 2009). The effective annual precipitation (P_e) is defined as the difference between annual precipitation and actual evapotranspiration. Each MDMC was plotted as Q_a, BF_a, and SR_a respectively against P_{ae}. In this way, the effects of climate variability on each streamflow component can be eliminated (Wei and Zhang, 2010; Zhang et al., 2017c). For a period with no or little forest disturbance, a straight line between each cumulative annual streamflow component and P_{ae} is expected, which is considered the reference. Break points between periods with different slopes can be identified on MDMC if there are significant influences from non-climatic variables, such as forest disturbance in our study. The Pettitt break point test was used to test the statistical significance of break points (Pettitt, 1979). Before implementation of the Pettitt test, any autocorrelation existing in the slope of MDMC must be removed, following the method by Yue et al. (2002). The nonparametric Mann-Whitney U test Z statistic was further adopted to compare the statistical difference of the MDMC slopes before and after each break point (Liu et al., 2015a). Once the statistical difference of each break point was confirmed, the whole study period was subsequently divided into reference (before the break point) and disturbance (after the break point) periods. The baseline relationship in the reference period was therefore employed to predict each cumulative annual streamflow component for the respective disturbance period. The difference between each observed and predicted annual streamflow component was treated as the deviations caused by forest disturbance (ΔQ_f). Thus, the deviations caused by climate variability on each annual streamflow component can be determined as:

$$\Delta Q_c = \Delta Q - \Delta Q_f \tag{3}$$

where, ΔQ, ΔQ_f, and ΔQ_c are the deviations of each annual streamflow component between disturbance and reference periods, annual flow deviations caused by forest disturbance, and annual flow deviations caused by climate variability, respectively.

Thus, the relative contributions of forest disturbance and climate variability to streamflow components can be calculated as:

$$R_f = \frac{|\Delta Q_f|}{|\Delta Q_f| + |\Delta Q_c|} \times 100\% \tag{4}$$

$$R_c = \frac{|\Delta Q_c|}{|\Delta Q_f| + |\Delta Q_c|} \times 100\% \tag{5}$$

where, R_f and R_c are the relative contributions of forest disturbance and climatic variability to annual streamflow components, respectively (Wei and Zhang, 2010).

In this study, monthly potential evapotranspiration (PET) was estimated through the Priestley-Taylor method (Eq. (6)) and Hamon method (Eqs. (7) and (8)). The average monthly PET values from two methods were then used to calculate actual evapotranspiration (ET) by Eqs. (9) and (10). The final monthly ET estimates were averaged values from Eqs. (9) and (10). Finally, the monthly PET and ET were aggregated to derive annual values.

$$PET = \alpha\left[\frac{\Delta}{\Delta+\gamma}\frac{R_n}{\lambda} - \frac{G}{\lambda}\right] \tag{6}$$

$$PET = 0.1651 \times D \times K \times 216.7 \times \frac{V_s}{(T+273.3)} \tag{7}$$

$$V_s = 6.108 \times \exp\left(17.27 \times \frac{T}{T+237.3}\right) \tag{8}$$

$$ET = \{P[1-\exp(-PET/P)] \times PET \times \tanh(P/PET)\}^{0.5} \tag{9}$$

$$ET = P\frac{1+\omega(PET/P)}{1+\omega(PET/P)+P/PET} \tag{10}$$

where, Eqs. (6)–(10) are the methods of Priestley-Taylor (Priestley and Taylor, 1972), Hamon (Zhou et al., 2015), Budyko (Budyko, 1974), and Zhang (Zhang et al., 2001), respectively. α is constant of the Priestley-Taylor ($\alpha = 1.26$ in this study). Δ is slope of the vapor press curve (kPa °C^{-1}); γ is the psychrometric constant (kPa °C^{-1}); R_n is the net daily radiation at the evaporating surface (MJ m^{-2} day^{-1}); and G is soil flux into the ground (MJ m^{-2} day^{-1}). The calculation of the Priestley-Taylor followed the procedure provided in McMahon et al. (2013). For Hamon method, D is the time from sunrise to sunset in multiples of 12 h; K is the correction coefficient; and V_s is saturated vapor pressure. For Zhang's method, P is monthly precipitation (mm); ET is monthly actual evapotranspiration (mm); and w is the plant-available water coefficient ($w = 2$ was used for this study).

4. Results

4.1. Baseflow separation

The conductivities corresponding to the highest and lowest flow rates were determined as C_{ro} (64.3 µs cm^{-1}) on May 22, 2015, with a discharge of 74.1 $m^3\ s^{-1}$ and C_{bf} (271.3 µs cm^{-1}) on August 28, 2015, with a discharge of 1.9 $m^3\ s^{-1}$ (Fig. 3). The *BFI* calculated from the CMB method was 0.25, which was further used as the initial value of BFI_{max} for the RDF method. Paired α and BFI_{max} in the RDF method were finally determined as 0.90 and 0.27, respectively. The mean annual baseflow was 113.3 ± 35.6 mm, and the mean annual *BFI* was 0.27 ± 0.004 in 1954–2013. The baseflow in the USR watershed showed temporal variations with the lowest *BFI* of 0.21 during the snow-melting seasons, while the highest *BFI* of 0.37 was in July and August (Fig. 5).

4.2. Trends of hydrometeorological variables

For annual hydrometeorological variables over the study period, significant increasing trends ($P < .01$) were detected in annual T_{max}, T_{min}, and T_{mean} and *PET* in 1954–2013 (Table 2). No significant trends ($P > .05$) were found in annual *P*, *ET*, streamflow, and baseflow. Significant upward trends ($P < .05$) were detected in seasonal T_{min} and T_{mean}. Only a significant upward trend was identified in spring *ET* ($P < .01$), while no significant trends ($P > .05$) were found in the other seasons. Significant downward trends ($P < .05$) were found in summer streamflow and baseflow, while no significant trends ($P > .05$) were detected in the other seasonal flow variables. Results of the trend analyses indicated that climate variability, which was characterized by the increase in temperature and *PET*, may play a negative role in the changes of all streamflow components.

4.3. Cross-correlations between CECA and streamflow components

Cross-correlations analysis between the CECA and each streamflow component in Table 3 showed that forest disturbance and all streamflow components were significantly related ($P < .05$), suggesting that forest disturbance has significantly affected all

Table 3
Cross-correlations between cumulative equivalent clear-cut area (CECA) and streamflow components (the bolded numbers indicate the statistical correlations at the significant level of .05).

Hydrological variables	Cross-correlation		
	ARIMA Model	Coefficients	Lag
Annual streamflow	(0, 1, 1)	**0.287**	2
Annual baseflow	(0, 1, 1)	**0.294**	2
Annual surface runoff	(0, 1, 1)	**0.296**	2
ARIMA model for CECA (0, 2, 1)			

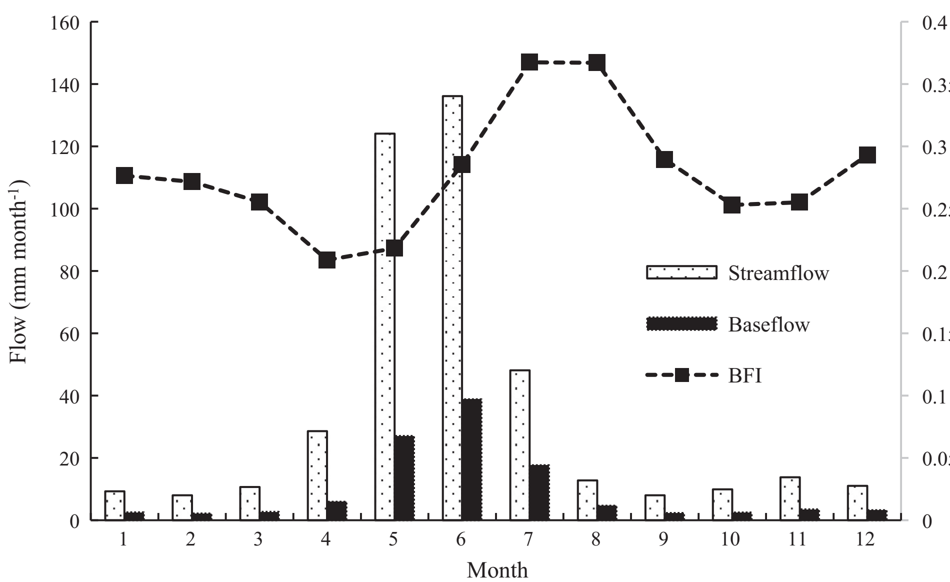

Fig. 5. Average monthly streamflow, baseflow, and baseflow index (*BFI*) in the Upper Similkameen River watershed from 1954 to 2013.

Table 2
Results of Mann-Kendall trend tests on hydrometeorological variables in the Upper Similkameen River watershed from 1954 to 2013.

Mann-Kendall trend test		T_{max}	T_{min}	T_{mean}	P	PET	ET	Q	BF
Annual	Z	**2.3**	**4.2**	**3.5**	0	**2.1**	1.4	−1.8	−1.8
	P	**0.02**	**<0.001**	**<0.001**	0.98	**0.04**	0.17	0.07	0.07
Spring	Z	1.5	**3**	**2.4**	**2.3**	1.7	**2.8**	−0.2	0
	P	0.14	**0.003**	**0.02**	**0.02**	0.09	**0.005**	0.85	0.99
Summer	Z	1.9	**4.7**	**3**	−0.1	1.7	−0.1	**−2**	**−2.3**
	P	0.06	**<0.001**	**0.002**	0.94	0.08	0.94	**0.04**	**0.02**
Fall-Winter	Z	1.5	**2.6**	**2.1**	−0.9	1.6	1.6	−0.3	−0.2
	P	0.12	**0.01**	**0.04**	0.38	0.11	0.12	0.79	0.83

Note: T_{max}, T_{min}, and T_{mean} denote maximum, minimum, and mean temperatures, respectively; P: precipitation; PET: Potential evapotranspiration; ET: Evapotranspiration; Q: Streamflow; BF: Baseflow; Spring: March to May; Summer: June to September; Fall-Winter: January, February, and October to December (the bolded numbers indicate the statistical significance at the level of 0.05).

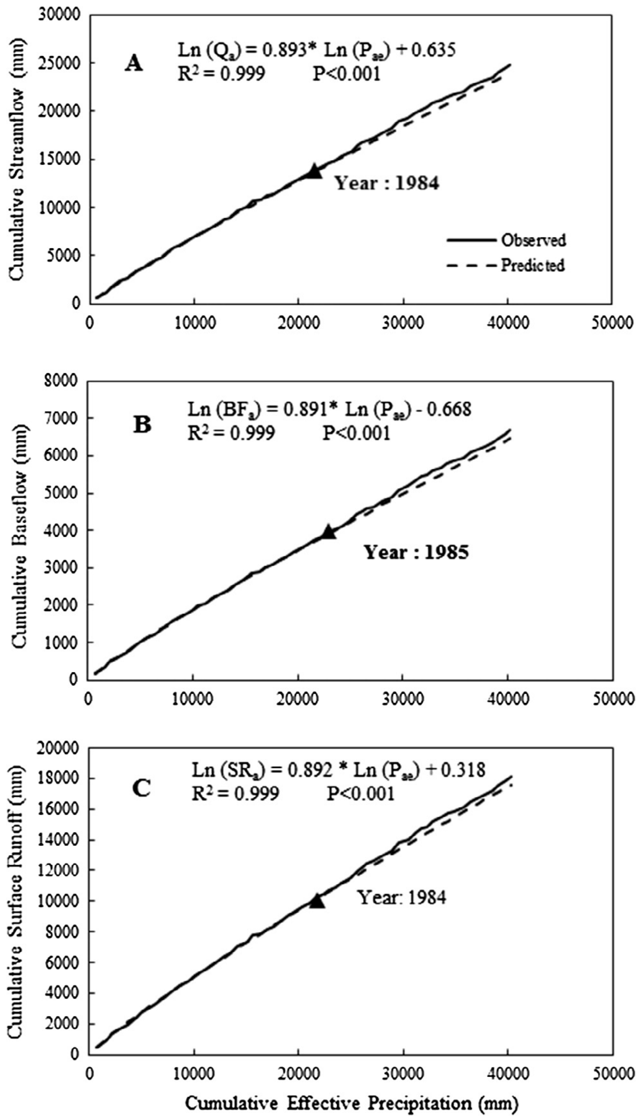

Fig. 6. A) Modified Double Mass Curve (MDMC) of cumulative annual streamflow (Q_a) against cumulative effective precipitation (P_{ae}); B) MDMC of cumulative annual baseflow (BF_a) against P_{ae}; and C) MDMC of cumulative annual surface runoff (SR_a) against P_{ae}. (Triangle indicates the year of break point occurred).

streamflow components. In addition, positive coefficients of cross-correlation indicated that forest disturbance significantly increased annual total streamflow, baseflow, and surface runoff in the study watershed in 1954–2013. It should be noted that the CECA was only calculated in Canada. Although the upper portion of the watershed is mainly located in the conservation parks of Canada and the USA, recent MPB infestation might have increased forest disturbance in these areas, which was not included in our analysis. Thus, our results on the relationship between the CECA and the streamflow components are conservative.

4.4. Quantification of the relative contributions of forest disturbance and climate variability to streamflow components

As shown in Fig. 6, one break point was detected for total streamflow, baseflow, and surface runoff, which occurred in 1984, 1985, and 1984, respectively. Additionally, Mann-Whitney *U* tests confirmed that the slopes of MDMCs before and after the break points were statistically different ($P < .001$) (Table 4). The break points coincided with the history of forest disturbance as the CECA increased from 7.8% in 1983 to 12.9% in 1985 (Fig. 4).

Forest disturbance increased annual streamflow, baseflow, and surface runoff of 27.7 ± 13.7 mm, 7.4 ± 3.6 mm, and 18.4 ± 12.9 mm, respectively, with its relative contributions to the changes in respective streamflow components being 27.0 ± 23.0%, 29.2 ± 23.1%, and 25.7 ± 23.4%, respectively. While climate variability reduced total streamflow, baseflow, and surface runoff by 74.9 ± 13.7 mm, 17.9 ± 3.6 mm, and 53.3 ± 12.9 mm, respectively, with its relative contributions to the changes in respective streamflow components being 73.0 ± 23.0%, 70.8 ± 23.1% and 73.1 ± 23.4%, respectively (Tables 5–7), respectively. Overall, the effects of climate variability on all streamflow components were much higher than those from forest disturbance, indicating the flow variations in the USR watershed were mainly caused by climate variability. The disturbance period was further divided into two sub-periods, including 1985–1998 and 1998–2013 based on the distinct change in the rate of forest disturbance (Fig. 4). The relative contribution of forest disturbance to all flow components showed temporal variations. For example, the relative contributions of forest disturbance to all streamflow components were higher in 1986–1994 than those in 1995–2013. In summary, our results demonstrated that climate variability played a more important role in the variations of all streamflow components in comparison to forest disturbance, but in the opposite direction.

5. Discussion

5.1. Baseflow separation

Our baseflow separation results showed that the average annual baseflow and *BFI* were 113.3 ± 35.6 mm year^{-1} (or 11.3% of average annual precipitation) and 0.27 ± 0.004 in 1954–2013, respectively. Our estimations of baseflow were comparable with groundwater recharge rates estimated by other studies in the region. For example, average annual recharge rates were 88 mm or 19.7% of precipitation in Vernon, Northern Okanagan, British Columbia (Liggett and Allen, 2010) and 77.8 ± 50.8 mm or 15.7% of precipitation in the Deep Creek watershed in North Okanagan (Assefa and Woodbury, 2013).

Several studies at the small watershed scale indicated that forest disturbance increased the conductivity in streams (Pike et al., 2010). This may lead to a concern over the assumption of the conductivity being temporally constant for applying the CMB method. In our study watershed, the long-term discrete conductivity (about twice per month) has been measured since 1967 (supplementary materials; Fig. S1). Our analysis using Kendall tau and Spearman rho's tests on the C_{ro}, C_{bf}, and C_q (the details of the calculations

Table 4
Results of break point tests for the MDMC slopes of streamflow components.

Flow components	Break Point (year)	Pettitt test		Mann-Whitney *U* test	
		K	P	Z	P
Streamflow	Year 1984	760	<0.001	−4.058	<0.001
Baseflow	Year 1985	783	<0.001	−6.197	<0.001
Surface runoff	Year 1984	543	0.005	−2.706	0.007

Table 5
Temporal variation of the relative contributions of forest disturbance and climate variability to annual streamflow in the Upper Similkameen River watershed from 1985 to 2013.

Periods	ΔQ (mm)	$ΔQ_f$ (mm)	$ΔQ_c$ (mm)	$ΔQ_f/Q$ (%)	$ΔQ_c/Q$ (%)	R_f (%)	R_c (%)	CECA (%)
1985–1998	−25.1	29.3 ± 14.5	−54.4 ± 14.5	7.3	−13.4	28.8 ± 31.3	65.0 ± 27.0	15.0
1999–2013	−61.1	23.9 ± 13.4	−85.1 ± 13.4	6.4	−22.6	22.0 ± 18.6	78.0 ± 18.6	28.2
1985–2013	−47.2	27.7 ± 13.7	−74.9 ± 13.7	7.1	−19.2	27.0 ± 23.0	73.0 ± 23.0	21.4

Note: ΔQ is the flow difference between the reference and disturbance period. $ΔQ_f$ and $ΔQ_c$ are the streamflow changes attributed to forest disturbance and climate variability, respectively. R_f and R_c are the relative contributions of forest disturbance and climate variability to streamflow.

Table 6
Temporal variation of the relative contributions of forest disturbance and climate variability to annual baseflow in the Upper Similkameen River watershed from 1986 to 2013 (acronyms are described in Table 5).

Periods	ΔBF (mm)	$ΔBF_f$ (mm)	$ΔBF_c$ (mm)	$ΔBF_f/BF$ (%)	$ΔBF_c/BF$ (%)	R_f (%)	R_c (%)	CECA (%)
1986–1998	−5.3	8.2 ± 3.8	−13.4 ± 3.8	7.4	12.0	37.8 ± 24.2	62.2 ± 24.2	15.2
1999–2013	−15.0	6.7 ± 3.5	−21.7 ± 3.5	6.6	21.4	23.5 ± 9.7	76.5 ± 9.7	28.2
1986–2013	−10.5	7.4 ± 3.6	−17.9 ± 3.6	7.0	16.9	29.2 ± 23.1	70.8 ± 23.1	21.7

Table 7
Temporal variation of the relative contributions of forest disturbance and climate variability to annual surface runoff in the Upper Similkameen River watershed from 1985 to 2013 (acronyms are described in Table 5).

Periods	ΔSR (mm)	$ΔSR_f$ (mm)	$ΔSR_c$ (mm)	$ΔSR_f/ΔSR$ (%)	$ΔSR_c/ΔSR$ (%)	R_f (%)	R_c (%)	CECA (%)
1985–1998	−18.7	19.5 ± 13.5	−38.3 ± 13.5	6.6	13.0	33.8 ± 25.7	65.5 ± 25.7	15.0
1999–2013	−45.1	15.6 ± 12.4	−60.7 ± 12.4	5.7	22.1	21.4 ± 9.5	78.6 ± 9.5	28.2
1985–2013	−34.9	18.4 ± 12.9	−53.3 ± 12.9	6.5	17.9	25.7 ± 23.4	73.1 ± 23.4	21.7

are provided in the supplementary materials, section 3 and Table S3) showed that no significant temporal trends were detected in those variables, indicating that cumulative forest disturbance did not cause a significant change in conductivity in the USR watershed (Table S3). Therefore, we believe that the effects of forest disturbance did not affect the applications of the CMB method in the USR watershed. In addition, Li et al. (2014) suggested that a minimum data requirement for the baseflow separation method is 6 months over a dry period. In this study, continuous conductivity data were collected for one year to minimize the possible uncertainties in the baseflow separation method. Furthermore, the RDF method has been proven to be an accurate baseflow separation method with a good estimation of BFI_{max} from a tracer method (Zhang et al., 2017a). In summary, the selected baseflow separation method (RDF) is sound for this study, and its application provides reliable estimates of baseflow or groundwater recharge in the study watershed.

5.2. The cumulative effects of forest disturbance on streamflow components

Over the disturbance periods, the average increments of annual total streamflow, baseflow, and surface runoff attributed to forest disturbance were 27.7 ± 13.7 mm, 7.4 ± 3.6 mm, and 18.4 ± 12.9 mm, respectively. Cumulative forest disturbance in the USR watershed has caused significant changes in all streamflow components, likely due to increasing soil water storage as a result of less evapotranspiration caused by forest disturbance. The USR watershed has a snow-melt dominated hydrological regime. After forest disturbance, more snow accumulation, and earlier and quicker melting are expected (Winkler et al., 2005), which consequently results in an increase in surface runoff and total streamflow. Meanwhile, forest disturbance also increases soil moisture and groundwater recharge, leading to more baseflow.

The impacts of forest disturbance on annual total streamflow, baseflow, and surface runoff have been investigated separately in previous studies. These studies consistently found that annual total streamflow was increased by forest disturbance in both small and large watersheds (Li et al., 2017; Zhang et al., 2017a). In contrast, the results of baseflow and surface runoff were inconsistent across different spatial scales. In small watersheds, a decrease in forest cover can increase baseflow or groundwater recharge (Table 1; Le Maitre et al., 1999; Smerdon et al., 2009), while in large watersheds, Ahiablame et al. (2017) found that every 1% increase in the agricultural land can lead to 0.2% decrease in baseflow. Using the SWAT model, Ma et al. (2009) showed that reforestation decreased surface runoff and total streamflow, but increased baseflow. Zhou et al. (2013) also found that surface runoff was increased of 11.3% while baseflow was decreased by 11.2% due to forest deduction and increase in urban area in Xitiaoxi Basin (1371 km^2), China. Those inconsistent responses may be attributed to different forest structures, altered soil conditions, and climatic regimes (Bruijnzeel, 2004; Liu et al., 2015b; Liu et al., 2016), highlighting that the effects of forest change on streamflow components are likely watershed-specific. It further demonstrates that focusing on one or two streamflow components might not provide a holistic picture of hydrological responses to forest or land cover changes.

Understanding the impacts of forest disturbance on baseflow has profound implications for managing groundwater resources. Dynamics of baseflow or groundwater recharge are critical for explaining the variations of groundwater storage and water quality in a watershed. For example, Zhang and Schilling (2006) found that elevated nitrate levels in streams were mainly from baseflow. Zhou et al. (2013) demonstrated that the expansion of urban area led to 11.3% increase in surface runoff and 11.2% decrease in baseflow. Such a pattern shift has important influences on droughts and consequently groundwater management. This also suggests that a full understanding of how various streamflow components respond to forest disturbance or land cover change can help in understanding and managing groundwater resources.

5.3. Relative contributions of forest disturbance and climate variability to streamflow components

Numerous studies have revealed that forest disturbance and climate variability played a similar role in total streamflow changes (Li et al., 2017). However, the relative contributions of forest dis-

turbance to total streamflow was only 27.0% with the CECA being 21.4% in the USR watershed, which was lower than those from other studies in the interior of British Columbia. For example, Zhang et al. (2017c) investigated the relative contributions of the forest disturbance to annual streamflow were 42.7% in the Willow River watershed (CECA of 23.8%), 40.4% in the Bake River watershed (CECA of 35.0%), 43.3% in the Moffat River watershed (CECA of 40.0%), and 50.4% in the Tulameen River watershed (CECA of 16.6%). This may be due to differences in climate regimes and levels of forest disturbance. The typical BC interior watersheds normally have a continental climate. However, the USR watershed has a mixed type of climate including a moist climate in the upper portion (mainly located in the conservation parks) and a relatively dry continental climate in the lower reaches of the watershed. This mixed type of climate may promote a larger influence of climate variability on total streamflow. Nevertheless, the effects of forest disturbance on total streamflow in the USR watershed should be considered when managing water resources and water-related functions.

Variations in the relative contributions of land cover change and climate variability to the streamflow components have been reported in the literature (Table 1). For example, all streamflow components were more sensitive to climate variability than to land cover change in the Heihe River basin (12,800 km^2), in Northwest China (Zhang et al., 2016) and in Xixian Basin, China (10,191 km^2) (Shi et al., 2013). Similarly, the application of the Variable Infiltration Capacity model in the Qingyi River watershed (13,263 km^2) showed that total streamflow and baseflow changes were mainly attributed to climate variability rather than land cover changes (Liu et al., 2013). Conversely, land cover played a more dominant role in the changes of all major streamflow components in the Kejie watershed (Ma et al., 2009) and Upper Du watershed (8961 km^2) (Huang et al., 2016) in China. Those contrasting results suggested large variations in hydrological responses were mainly due to the different magnitudes of disturbance and climate variability across watersheds.

Forest disturbance and climate variability can have offsetting or additive effects on annual streamflow (Wei and Zhang, 2010; Zhang et al., 2008, 2012; Li et al., 2017; Wei et al., 2017). Our study indicated that the effects of forest disturbance and climate variability offset each other on all streamflow components. Similarly, the offsetting effects of forest disturbance and climate variability on all streamflow components have been detected in the Be River catchment using SWAT (Khoi and Suetsugi, 2014). In contrast, Liu et al. (2013) detected that land cover changes enhanced the impacts of climate variability on all streamflow components in the Qingyi River watershed, China. Normally, offsetting effects can lead to less variations in water resource, while additive effects can cause river flows to either increase (e.g., higher chances of floods) or decrease (e.g., higher chances of droughts) (Li et al., 2017). Forest disturbance may increase annual streamflow, baseflow, and surface runoff, which can help to alleviate water stress in areas with water scarcity. However, the negative effects of forest disturbance on aquatic ecosystems, such as increasing turbidity, may overshadow any potential positive effects. Thus, forest disturbance, climate, and their interactions must be carefully managed in order to sustain water supply for human use as well as for aquatic functioning.

5.4. Recommendations and uncertainties

In this study, our MDMC framework was successfully applied to quantify the long-term cumulative effects of forest disturbance on all major streamflow components, which can be extended to other watershed studies. This study is the first application of this framework on annual baseflow and surface runoff. To successfully implement this methodology on all streamflow components, it is necessary to generate the relatively accurate baseflow data series. The objective tracer-based method was used for baseflow separation, which reduced the uncertainties in baseflow separation methods. To extend this method to other watersheds, long-term data on climate, streamflow, and forest change must be available. In addition, any selected watersheds must experience significant forest change (e.g., disturbance or reforestation) so that possible hydrological shifts can be detected.

There are several uncertainties in this study. First, the *PET* values were derived from the Priestley-Taylor method and Hamon method, based on the recommendation of Lu et al. (2005). In this study, we used the averaged *PET* values from two methods, which minimized some uncertainties introduced by adopting one method alone. However, various studies have demonstrated that the changes in surface humidity (Willett et al., 2008), vapor pressure, wind speed (McVicar et al., 2012), and net radiation (Wild, 2009) have impacts on evaporative demand and thus *PET*. Yet, these factors were not considered in the *PET* calculations in this study. Second, the changes in seasonal climate patterns and their effects on streamflow were not considered (Berghuijs et al., 2014; Shen et al., 2017). For instance, Berghuijs et al. (2014) revealed that precipitation shift from snow to rain leads to a decrease in streamflow. Third, possible feedbacks between forest change and climate (Ellison et al., 2012; Khanna et al., 2017) were not fully accounted for.

6. Conclusion

Quantifying the long-term and cumulative effects of forest disturbance and climate variability on streamflow components has rarely been reported in the literature. In this study, we concluded that forest disturbance significantly increased all streamflow components, while climatic variability decreased them in the Upper Similkameen River watershed. The relative contributions of climate variability to annual total streamflow, baseflow, and surface runoff were 75.6 ± 25.0%, 72.4 ± 24.6%, and 76.3 ± 76.3%, respectively, while the rest of the changes in all streamflow components were attributed to forest disturbance. Climate variability played a more important role than forest disturbance in all streamflow components, but in the opposite direction. These findings help water or watershed managers make informed decisions when coping with future forest and climate changes in the USR watershed so that aquatic functioning and water supply can be sustained.

Acknowledgements

We thank the British Columbia Ministry of Forests, Lands and Natural Resources Operations for providing forest inventory data. Thanks are also given to Environment Canada for their streamflow and conductivity data. The authors would also like to thank the Editor (Dr. Tim R. McVicar), Associate Editor (Dr. Shengping Wang), three anonymous reviewers for their constructive comments on the earlier version of the paper. The funding for supporting this project was provided by the Natural Sciences and Engineering Research Council of Canada (RGPIN-2015-06032) and the Regional District of Okanagan Similkameen through a contract.

Appendix A. Supplementary data

Supplementary data associated with this article can be found, in the online version, at https://doi.org/10.1016/j.jhydrol.2017.12.056.

References

Andréassian, V., 2004. Waters and forests: from historical controversy to scientific debate. J. Hydrol. 291 (1–2), 1–27. https://doi.org/10.1016/j.jhydrol.2003.12.015.

Ahiablame, L., Sheshukov, A.Y., Rahmani, V., Moriasi, D., 2017. Annual baseflow variations as influenced by climate variability and agricultural land use change in the Missouri River Basin. J. Hydrol. 551, 188–202. https://doi.org/10.1016/j.jhydrol.2017.05.055.

Assefa, K.A., Woodbury, A.D., 2013. Transient, spatially varied groundwater recharge modeling. Water Resour. Res. 49 (8), 4593–4606. https://doi.org/10.1002/wrcr.20332.

Barnett, S., 1990. Effect of land clearance in the mallee region on river Murray salinity and land salinisation. BMR J. Aust. Geol. Geophys. 11 (2), 205–208.

Bent, G.C., 2001. Effects of forest-management activities on runoff components and ground-water recharge to Quabbin Reservoir, central Massachusetts. For. Ecol. Manage. 143 (1), 115–129. https://doi.org/10.1016/S0378-1127(00)00511-9.

Berghuijs, W.R., Woods, R.A., Hrachowitz, M., 2014. A precipitation shift from snow towards rain leads to a decrease in streamflow. Nat. Clim. Change 4 (7), 583–586. https://doi.org/10.1038/Nclimate2246.

Bliss, C., Comerford, N., 2002. Forest harvesting influence on water table dynamics in a Florida flatwoods landscape. Soil Sci. Soc. Am. J. 66 (4), 1344–1349.

Brown, A.E., Zhang, L., McMahon, T.A., Western, A.W., Vertessy, R.A., 2005. A review of paired catchment studies for determining changes in water yield resulting from alterations in vegetation. J. Hydrol. 310 (1), 28–61. https://doi.org/10.1016/j.jhydrol.2004.12.010.

Bruijnzeel, L.A., 2004. Hydrological functions of tropical forests: not seeing the soil for the trees? Agric. Ecosyst. Environ. 104 (1), 185–228. https://doi.org/10.1016/j.agee.2004.01.015.

Budyko, M.I., 1974. In: Climate and Life, Int. Geophys. Series. Academic Press, New York and London, p. 508.

Calder, I.R., Hall, R., Adlard, P.G., 1992. Growth and Water Use of Forest Plantations. John Wiley and Sons Inc, New York, NY (United States).

Cao, W.Z., Bowden, W.B., Davie, T., Fenemor, A., 2009. Modelling impacts of land cover change on critical water resources in the Motueka river catchment, New Zealand. Water Resour. Manage. 23 (1), 137–151. https://doi.org/10.1007/s11269-008-9268-2.

Cook, P.G., Walker, G.R., Jolly, I.D., 1989. Spatial variability of groundwater recharge in a semiarid region. J. Hydrol. 111 (1–4), 195–212. https://doi.org/10.1016/0022-1694(89)90260-6.

Dubé, S., Plamondon, A.P., Rothwell, R.L., 1995. Watering up after clear-cutting on forested wetlands of the St. Lawrence lowland. Water Resour. Res. 31 (7), 1741–1750. https://doi.org/10.1029/95WR00427.

Eckhardt, K., 2005. How to construct recursive digital filters for baseflow separation. Hydrol. Process. 19 (2), 507–515. https://doi.org/10.1002/hyp.5675.

Ellison, D., Futter, M.N., Bishop, K., 2012. On the forest cover-water yield debate: from demand- to supply-side thinking. Global Change Biol. 18 (3), 806–820. https://doi.org/10.1111/j.1365-2486.2011.02589.x.

Evans, J., Prepas, E., Devito, K., Kotak, B., 2000. Phosphorus dynamics in shallow subsurface waters in an uncut and cut subcatchment of a lake on the Boreal Plain. Can. J. Fish. Aquat. Sci. 57 (S2), 60–72. https://doi.org/10.1139/f00-123.

Fannin, R., Jaakkola, J., Wilkinson, J., Hetherington, E., 2000. Hydrologic response of soils to precipitation at Carnation Creek, British Columbia, Canada. Water Resour. Res. 36 (6), 1481–1494. https://doi.org/10.1029/2000WR900027.

Farley, K.A., Jobbagy, E.G., Jackson, R.B., 2005. Effects of afforestation on water yield: a global synthesis with implications for policy. Global Change Biol. 11 (10), 1565–1576. https://doi.org/10.1111/j.1365-2486.2005.01011.x.

Hetherington, 1998. Watershed hydrology. In: Hogan, D.L., Tschaplinski, P.J., Chatwin, S. (Eds.), Carnation Creek and Queen Charlotte Islands fish/forestry workshop: Applying 20 Years of Coastal Research to Management Solutions. BC Ministry of Forests, Victoria, BC, pp. 33–40.

Huang, X.-D., Shi, Z.-H., Fang, N.-F., Li, X., 2016. Influences of land use change on baseflow in mountainous watersheds. Forests 7 (1), 16. https://doi.org/10.3390/f7010016.

Khanna, J., Medvigy, D., Fueglistaler, S., Walko, R., 2017. Regional dry-season climate changes due to three decades of Amazonian deforestation. Nat. Clim. Change 7 (3), 200–2004. https://doi.org/10.1038/Nclimate3226.

Khoi, D.N., Suetsugi, T., 2014. The responses of hydrological processes and sediment yield to land-use and climate change in the Be River Catchment, Vietnam. Hydrol. Process. 28 (3), 640–652. https://doi.org/10.1002/hyp.9620.

Leduc, C., Favreau, G., Schroeter, P., 2001. Long-term rise in a Sahelian water-table: the continental terminal in South-West Niger. J. Hydrol. 243 (1–2), 43–54. https://doi.org/10.1016/S0022-1694(00)00403-0.

Le Maitre, D.C., Scott, D.F., Colvin, C., 1999. A review of information on interactions between vegetation and groundwater. Water SA 25 (2), 137–152.

Li, Q., Xing, Z., Danielescu, S., Li, S., Jiang, Y., Meng, F., 2014. Data requirements for using combined conductivity mass balance and recursive digital filter method to estimate groundwater recharge in a small watershed, New Brunswick, Canada. J. Hydrol. 511, 658–664. https://doi.org/10.1016/j.jhydrol.2014.01.073.

Li, Q., Wei, X., Zhang, M., Liu, W., Fan, H., Zhou, G., Giles-Hansen, K., Liu, S., Wang, Y., 2017. Forest cover change and water yield in large forested watersheds: a global synthetic assessment. Ecohydrology. 10.1002/eco.1838.

Liggett, J.E., Allen, D.M., 2010. Comparing approaches for modeling spatially distributed direct recharge in a semi-arid region (Okanagan Basin, Canada). Hydrogeol. J. 18 (2), 339–357. https://doi.org/10.1007/s10040-009-0512-5.

Liu, W., Wei, X., Liu, S., Liu, Y., Fan, H., Zhang, M., Yin, J., Zhan, M., 2015a. How do climate and forest changes affect long-term streamflow dynamics? A case study in the upper reach of Poyang River basin. Ecohydrology 8 (1), 46–57. https://doi.org/10.1002/eco.1486.

Liu, W., Wei, X., Fan, H., Guo, X., Liu, Y., Zhang, M., Li, Q., 2015b. Response of flow regimes to deforestation and reforestation in a rain-dominated large watershed of subtropical China. Hydrol. Process. 29 (24), 5003–5015. https://doi.org/10.1002/hyp.10459.

Liu, W., Wei, X., Li, Q., Fan, H., Duan, H., Wu, J., Giles-Hansen, K., Zhang, H., 2016. Hydrological recovery in two large forested watersheds of southeastern China: the importance of watershed properties in determining hydrological responses to reforestation. Hydrol. Earth Syst. Sci. 20 (12), 4747–4756. https://doi.org/10.5194/hess-20-4747-2016.

Liu, Y., Zhang, X., Xia, D., You, J., 2013. Impacts of land-use and climate changes on hydrologic processes in the Qingyi River Watershed, China. J. Hydrol. Eng. 18 (11), 1495–1512. https://doi.org/10.1061/(Asce)He.1943-5584.0000485.

Lu, J.B., Sun, G., McNulty, S.G., Amatya, D.M., 2005. A comparison of six potential evapotranspiration methods for regional use in the southeastern United States. J. Am. Water Resour. Assoc. 41 (3), 621–633. https://doi.org/10.1111/j.1752-1688.2005.tb03759.x.

Ma, X., Xu, J.C., Luo, Y., Aggarwal, S.P., Li, J.T., 2009. Response of hydrological processes to land-cover and climate changes in Kejie watershed, south-west China. Hydrol. Process. 23 (8), 1179–1191. https://doi.org/10.1002/hyp.7233.

Marcotte, P., Roy, V., Plamondon, A.P., Auger, I., 2008. Ten-year water table recovery after clearcutting and draining boreal forested wetlands of eastern Canada. Hydrol. Process. 22 (20), 4163–4172. https://doi.org/10.1002/hyp.7020.

Matsubayashi, U., Velasquez, G.T., Takagi, F., 1993. Hydrograph separation and flow-analysis by specific electrical conductance of water. J. Hydrol. 152 (1–4), 179–199. https://doi.org/10.1016/0022-1694(93)90145-Y.

McMahon, T.A., Peel, M.C., Lowe, L., Srikanthan, R., McVicar, T.R., 2013. Estimating actual, potential, reference crop and pan evaporation using standard meteorological data: a pragmatic synthesis. Hydrol. Earth Syst. Sci. 17 (4), 1331–1363. https://doi.org/10.5194/hess-17-1331-2013.

McVicar, T.R. et al., 2012. Global review and synthesis of trends in observed terrestrial near-surface wind speeds: implications for evaporation. J. Hydrol. 416, 182–205. https://doi.org/10.1016/j.jhydrol.2011.10.024.

Megahan, W.F., Clayton, J.L., 1983. Tracing subsurface flow on roadcuts on steep, forested slopes. Soil Sci. Soc. Am. J. 47 (6), 1063–1067.

Miller, M.P., Susong, D.D., Shope, C.L., Heilweil, V.M., Stolp, B.J., 2014. Continuous estimation of baseflow in snowmelt-dominated streams and rivers in the Upper Colorado River Basin: a chemical hydrograph separation approach. Water Resour. Res. 50 (8), 6986–6999. https://doi.org/10.1002/2013WR014939.

Mishra, V., Cherkauer, K.A., Niyogi, D., Lei, M., Pijanowski, B.C., Ray, D.K., Bowling, L. C., Yang, G., 2010. A regional scale assessment of land use/land cover and climatic changes on water and energy cycle in the upper Midwest United States. Int. J. Climatol. https://doi.org/10.1002/joc.2095.

Mitchell, T.D., Jones, P.D., 2005. An improved method of constructing a database of monthly climate observations and associated high-resolution grids. Int. J. Climatol. 25 (6), 693–712. https://doi.org/10.1002/joc.1181.

Nepstad, D.C., de Carvalho, C.R., Davidson, E.A., Jipp, P.H., 1994. The role of deep roots in the hydrological and carbon cycles of Amazonian forests and pastures. Nature 372 (6507), 666.

Peck, A., Williamson, D., 1987. Effects of forest clearing on groundwater. J. Hydrol. 94 (1), 47–65. https://doi.org/10.1016/0022-1694(87)90032-1.

Pettitt, A.N., 1979. A non-parametric approach to the change-point problem. J. R. Stat. Soc. Ser. C 28, 126–135.

Pike, R.G., Feller, M.C., Stednick, J.D., Rieberger, K.J., Carver, M., 2010. Water quality and forest management, Compendium of forest hydrology and geomorphology in British Columbia. BC Ministry of Forests and Range, Forest Science Program, Victoria, BC, and FORREX Forum for Research and Extension in Natural Resources, Kamloops, BC. Land Management Handbook, Citeseer.

Pojar, J., Klinka, K., Meidinger, D.V., 1987. Biogeoclimatic ecosystem classification in British-Columbia. For. Ecol. Manage. 22 (1–2), 119–154. https://doi.org/10.1016/0378-1127(87)90100-9.

Pothier, D., Prévost, M., Auger, I., 2003. Using the shelterwood method to mitigate water table rise after forest harvesting. For. Ecol. Manage. 179 (1), 573–583. https://doi.org/10.1016/S0378-1127(02)00530-3.

Priestley, C., Taylor, R., 1972. On the assessment of surface heat flux and evaporation using large-scale parameters. Mon. Weather Rev. 100 (2), 81–92.

Salama, R., Farrington, P., Bartle, G., Watson, G., 1993. The chemical evolution of groundwater in a first-order catchment and the process of salt accumulation in the soil profile. J. Hydrol. 143 (3–4), 233–258. https://doi.org/10.1016/0022-1694(93)90194-E.

Schofield, N., Bari, M., 1991. Valley reforestation to lower saline groundwater tables-Results from Stene Farm, Western-Australia. Soil Res. 29 (5), 635–650. https://doi.org/10.1071/SR9910635.

Scott, D.F., Lesch, W., 1997. Streamflow responses to afforestation with Eucalyptus grandis and Pinus patula and to felling in the Mokobulaan experimental catchments, South Africa. J. Hydrol. 199 (3–4), 360–377. https://doi.org/10.1016/S0022-1694(96)03336-7.

Shen, Q., Cong, Z., Lei, H., 2017. Evaluating the impact of climate and underlying surface change on runoff within the Budyko framework: a study across 224 catchments in China. J. Hydrol. 554, 251–262. https://doi.org/10.1016/j.jhydrol.2017.09.023.

Shi, P. et al., 2013. Effects of land-use and climate change on hydrological processes in the Upstream of Huai River, China. Water Resour. Manage. 27 (5), 1263–1278. https://doi.org/10.1007/s11269-012-0237-4.
Stednick, J.D., 1996. Monitoring the effects of timber harvest on annual water yield. J. Hydrol. 176 (1–4), 79–95. https://doi.org/10.1016/0022-1694(95)02780-7.
Stewart, M., Cimino, J., Ross, M., 2007. Calibration of base flow separation methods with streamflow conductivity. Ground Water 45 (1), 17–27. https://doi.org/10.1111/j.1745-6584.2006.00263.x.
Summit (Summit Environmental Consultants Inc.), 2011. Similkameen River Project, Part 1. Scoping Report. Available at: http://www.rdosmaps.bc.ca/min_bylaws/es/public_works/svwp/svpswater.pdf (accessed 26.06.17).
Smerdon, B.D., Redding, T., Beckers, J., 2009. An overview of the effects of forest management on groundwater hydrology. J. Ecosyst. Manage. 10 (1).
Urie, D.H., 1971. Estimated groundwater yield following strip cutting in pine plantations. Water Resour. Res. 7 (6), 1497–1510. https://doi.org/10.1029/WR007i006p01497.
Xu, X., Scanlon, B.R., Schilling, K., Sun, A., 2013. Relative importance of climate and land surface changes on hydrologic changes in the US Midwest since the 1930s: implications for biofuel production. J. Hydrol. 497, 110–120. https://doi.org/10.1016/j.jhydrol.2013.05.041.
Wang, T., Hamann, A., Spittlehouse, D., Carroll, C., 2016. Locally downscaled and spatially customizable climate data for historical and future periods for North America. PLoS One 11 (6), e0156720. https://doi.org/10.1371/journal.pone.0156720.
Wei, X.H., Liu, W.F., Zhou, P.C., 2013. Quantifying the relative contributions of forest change and climatic variability to hydrology in large watersheds: a critical review of research methods. Water-SUI 5 (2), 728–746. https://doi.org/10.3390/W5020728.
Wei, X., Li, Q., Zhang, M., Giles-Hansen, K., Liu, W., Fan, H., Wang, Y., Zhou, G., Piao, S., Liu, S., 2017. Vegetation cover—another dominant factor in determining global water resources in forested regions. Glob Change Biol., 1–10 https://doi.org/10.1111/gcb.13983.
Wei, X.H., Zhang, M.F., 2010. Quantifying streamflow change caused by forest disturbance at a large spatial scale: a single watershed study. Water Resour. Res. 46. https://doi.org/10.1029/2010wr009250.
Wild, M., 2009. Global dimming and brightening: a review. J. Geophys. Res. Atmos. 114, D00D16. https://doi.org/10.1029/2008JD011470.
Willett, K.M., Jones, P.D., Gillett, N.P., Thorne, P.W., 2008. Recent changes in surface humidity: development of the HadCRUH dataset. J. Clim. 21 (20), 5364–5383. https://doi.org/10.1175/2008JCLI2274.1.
Winkler, R.D., Spittlehouse, D.L., Golding, D.L., 2005. Measured differences in snow accumulation and melt among clearcut, juvenile, and mature forests in southern British Columbia. Hydrol. Process. 19 (1), 51–62. https://doi.org/10.1002/hyp.5757.
Yao, Y., Cai, T., Wei, X., Zhang, M., Ju, C., 2012. Effect of forest recovery on summer streamflow in small forested watersheds, Northeastern China. Hydrol. Process. 26 (8), 1208–1214.
Yue, S., Pilon, P., Phinney, B., Cavadias, G., 2002. The influence of autocorrelation on the ability to detect trend in hydrological series. Hydrol. Process. 16 (9), 1807–1829. https://doi.org/10.1002/hyp.1095.
Zhang, L., Dawes, W.R., Walker, G.R., 2001. Response of mean annual evapotranspiration to vegetation changes at catchment scale. Water Resour. Res. 37 (3), 701–708. https://doi.org/10.1029/2000wr900325.
Zhang, L., Nan, Z.T., Xu, Y., Li, S., 2016. Hydrological impacts of land use change and climate variability in the headwater region of the Heihe River Basin, Northwest China. PLoS One 11 (6). https://doi.org/10.1371/journal.pone.0158394.
Zhang, M.F., Wei, X.H., Sun, P.S., Liu, S.R., 2012. The effect of forest harvesting and climatic variability on runoff in a large watershed: the case study in the Upper Minjiang River of Yangtze River basin. J. Hydrol. 464, 1–11. https://doi.org/10.1016/j.jhydrol.2012.05.050.
Zhang, M.F., Wei, X.H., 2014. Contrasted hydrological responses to forest harvesting in two large neighbouring watersheds in snow hydrology dominant environment: implications for forest management and future forest hydrology studies. Hydrol. Process. 28 (26), 6183–6195. https://doi.org/10.1002/Hyp.10107.
Zhang, J., Zhang, Y.Q., Song, J.X., Cheng, L., 2017a. Evaluating relative merits of four baseflow separation methods in Eastern Australia. J. Hydrol. 549, 252–263. https://doi.org/10.1016/j.jhydrol.2017.04.004.
Zhang, M.F., Liu, N., Harper, R., Li, Q., Liu, K., Wei, X., Ning, D., Hou, Y., Liu, S., 2017b. A global review on hydrological responses to forest change across multiple spatial scales: importance of scale, climate, forest type, and hydrological regime. J. Hydrol. 546, 44–59. https://doi.org/10.1016/j.jhydrol.2016.12.040.
Zhang, M.F., Wei, X.H., Li, Q., 2017c. Do the hydrological responses to forest disturbance in large watersheds vary along climatic gradients in the interior of British Columbia, Canada? Ecohydrology. https://doi.org/10.1002/eco.1840.
Zhang, R.G., Li, Q., Chow, T.L., Li, S., Danielescu, S., 2013. Baseflow separation in a small watershed in New Brunswick, Canada, using a recursive digital filter calibrated with the conductivity mass balance method. Hydrol. Process. 27 (18), 2659–2665. https://doi.org/10.1002/hyp.9417.
Zhang, X., Zhang, L., Zhao, J., Rustomji, P., Hairsine, P., 2008. Responses of streamflow to changes in climate and land use/cover in the Loess Plateau, China. Water Resour. Res. 44 (7).
Zhang, Y.K., Schilling, K.E., 2006. Increasing streamflow and baseflow in Mississippi River since the 1940s: effect of land use change. J. Hydrol. 324 (1–4), 412–422. https://doi.org/10.1016/j.jhydrol.2005.09.033.
Zheng, H., Zhang, L., Zhu, R., Liu, C., Sato, Y., Fukushima, Y., 2009. Responses of streamflow to climate and land surface change in the headwaters of the Yellow River Basin. Water Resour. Res. 45. https://doi.org/10.1029/2007wr006665.
Zhou, F., Xu, Y., Chen, Y., Xu, C.Y., Gao, Y., Du, J., 2013. Hydrological response to urbanization at different spatio-temporal scales simulated by coupling of CLUE-S and the SWAT model in the Yangtze River Delta region. J. Hydrol. 485, 113–125. https://doi.org/10.1016/j.jhydrol.2012.12.040.
Zhou, G., Wei, X., Chen, X., Zhou, P., Liu, X., Xiao, Y., Sun, G., Scott, D.F., Zhou, S., Han, L., Su, Y., 2015. Global pattern for the effect of climate and land cover on water yield. Nat. Commun. 6. https://doi.org/10.1038/Ncomms6918.